Cancer Management and Research

Elevate Series

Open Access Full Text Article

ORIGINAL RESEARCH

The Role of AHCY Expression in Bladder Urothelial Carcinoma: A Bioinformatics and Experimental Analysis

Shaorui Niu[1], Xiaozhe Zheng[1], Yuyang Yao[1], Yue Dong[2], Yupan Hu[3], Zhiyang Xiao[1], Jiaxue Yang[1], Chengli Jiang[1], Xin Zou[4], Zihao Zou[5], Pang Yang[1]

[1]Jiangxi Key Laboratory of Cancer Metastasis and Precision Treatment, Central Laboratory, The First Hospital of Nanchang, The Third Affiliated Hospital of Nanchang University, Nanchang, People's Republic of China; [2]Zhejiang Provincial Clinical Research Center for Obstetrics and Gynecology, Department of Obstetrics and Gynecology, The Second Affiliated Hospital of Wenzhou Medical University, Wenzhou, People's Republic of China; [3]Fuzhou Medical College of Nanchang University, Fuzhou City, Jiangxi Province, People's Republic of China; [4]Clinical Medical College, Ningxia Medical University, Yinchuan, Ningxia Province, People's Republic of China; [5]Department of Orthopaedic Surgery, Fourth Hospital, Harbin Medical University, Harbin, People's Republic of China

Correspondence: Pang Yang, Email pyang392@163.com

Background: Although adenosylhomocysteinase (AHCY) is crucial to the oncogenesis and growth of some cancers, it is unknown how this affects bladder urothelial carcinoma (BLCA). Investigating the variations in AHCY expression in BLCA and examining the relationship between AHCY expression and BLCA patient prognosis were the goals of this investigation.

Methods: By leveraging The Cancer Genome Atlas (TCGA) database, we undertook a meticulous examination of AHCY expression levels, juxtaposing them between BLCA and normal tissues. Subsequently, Kaplan-Meier analysis and COX regression and nomogram was used to assess the effect of AHCY on the survival of BLCA patients. We further elaborated on the possible enriched pathways of AHCY and its immune relevance. In addition, we employed si-RNA technology to downregulate the AHCY gene expression and subsequently utilized quantitative real-time PCR (qRT-PCR), CCK-8, cell scratch assays, and Transwell migration assays to validate the pivotal role of AHCY in BLCA.

Results: The expression of AHCY was associated with various types of malignancies (including BCLA). In BLCA cancer tissues, there was an observed upregulation of AHCY expression in comparison to paracancerous tissues. Increased expression of AHCY was linked to decreased overall survival (OS), clinical stage, N stage, and T stage in individuals with BLCA. The functional enrichment of AHCY related genes mainly involves biological processes such as rRNA metabolic processes, proteasome activity, and cell cycle regulation, etc. Furthermore, AHCY showed significant associations with m6A related genes and infiltration of immune cells (Especially for Th2 cells and T-gd lymphocytes). In vitro functional experiments substantiated that the inhibition of AHCY effectively suppresses the growth, migration, and invasion of bladder cancer cells.

Conclusion: This study provides novel insights into the role of AHCY in BLCA, which holds significant potential to contribute towards advancing the diagnosis and treatment of BLCA in the future.

Keywords: adenosylhomocysteinase, bladder urothelial carcinoma, biomarker, immune infiltration, prognosis

Introduction

The enzyme known as S-adenosylhomocysteine hydrolase (AHCY) is highly conserved across various living organisms.[1–3] In recent years, burgeoning reports have elucidated the association between AHCY and various malignancies, including colorectal cancer, prostate cancer, and glioblastoma.[4,5] However, the role of AHCY in bladder urothelial carcinoma (BLCA) remains unexplored. BLCA ranks as the tenth most prevalent malignant neoplasm globally, with an annual incidence of 573,000 new cases and causing 212,536 fatalities.[6] Despite significant advancements in BLCA treatment, the general outlook for patients with this condition remains unfavorable.[7] Consequently, a comprehensive investigation into the intricate molecular mechanisms underlying BLCA initiation and progression is of paramount importance.

Received: 12 September 2024
Accepted: 10 March 2025
Published: 21 March 2025

The tumor microenvironment (TME), a complex and dynamic cellular milieu, serves as the breeding ground for tumor proliferation, comprising an extensive array of intricate components. The prognosis of bladder cancer is strongly associated with varying levels of immune cell infiltration in the TME.[8–10] Indeed, a large of evidence suggests that the dysregulation of N6-methyladenosine (m6A) RNA methylation, a process in which AHCY plays a key role, is a significant factor in the genesis and advancement of numerous cancer types.[11,12] In recent times, a novel immune system escape mechanism reliant on m6A has been identified in BLCA cells, hence presenting a promising avenue for the development of BLCA immunotherapy.[13] Currently, there is a lack of available literature regarding the correlation between AHCY and tumor immune invasion, as well as the impact of m6A change.

This work aimed to enhance comprehension of the function of the AHCY gene in BLCA by examining the expression level of AHCY in BLCA utilizing data obtained from publicly available sources. And use cell experiment to validate the pivotal role of AHCY in BLCA. The results of our study offer support for the involvement of AHCY in the incidence and prognosis of BLCA, and have the potential to uncover biomarkers that may be used for predicting and treating BLCA.

Materials and Methods

Ethical Approval and Consent to Participate

This study was approved by the ethical committee of The First Hospital of Nanchang (Nanchang, China) (Ethical approval code: IIT2024023). The large-scale GWAS data used in our analysis which were publicly available were reported by human participants collected from several previous studies. In all original research, informed consent was obtained from all participants and the data were approved by the institutional review committee in the respective studies.

Data Sources

The mRNA expression profiles, in conjunction with pertinent clinical data downloaded from The Cancer Genome Atlas (TCGA) database and the Genotype-Tissue Expression (GTEx) database. The amplification and mutation statuses of the AHCY gene were provided by the cBioPortal platform.

Survival Analysis

The GEPIA database and the ggplot2 package were employed to conduct a comprehensive analysis of the impact of AHCY expression on the overall survival (OS) and disease-free survival (DFS) among patients with BLCA.

Construction and Evaluation of Nomogram

The association of the clinicopathological variables and the expression of AHCY with healing in BLCA patients was investigated by Cox regression analysis. A nomogram was constructed to predict survival probabilities at 1, 3, and 5-year intervals for BLCA patients.

Correlation and Gene Set Enrichment Analysis

To gain insights into the potential biological processes and pathways associated with AHCY, a correlation study was conducted utilizing the data collected by TCGA. This research comprised examining the relationship between AHCY and other mRNAs in BLCA. The Genome Ontology (GO) and Kyoto Encyclopedia of Genes and Genomes (KEGG) enrichment analysis was performed for these genes.

Relationship Between AHCY Expression Level and m6A Modification in BLCA

We performed spearman correlation analysis between AHCY and the expression level of m6A modification genes (including YTHDF1, YTHDF2, YTHDF3, YTHDC1, YTHDC2, WTAP, and RBM15, etc). Furthermore, the study also included the genes RBM15B, ZC3H13, HNRNPC, METTL14, METTL3, IGF2BP1, IGF2BP2, IGF2BP3, RBMX, HNRNPA2B1, VIRMA, FTO, and ALKBH5. The correlation analysis between these genes was adeptly performed using the sophisticated Corlot software tool.

Immune Landscape Analysis

The CIBERSORT algorithm, a method for quantifying immune cell infiltration, was employed to analyse the distribution of 22 subtypes of immune cells in the TCGA cohort, including the total count of immune cells. The ESTIMATE algorithm was employed to compute the matrix score. Additionally, TME was then examined in more detail.

Cell Culture

T24 and UMUC3 cells were sustained in DMEM, which was supplemented with 10% fetal bovine serum (FBS), while J82 and 5637 cells were cultured in RPMI 1640 medium, also containing 10% FBS. All cultures were incubated in an environment characterized by saturated humidity at 37°C with 5% CO2. In contrast, the normal bladder cell line SV-HUC-1, owing to its distinct growth requirements, was cultured in F-12K medium, which included 10% bovine serum and 1% penicillin-streptomycin, and maintained at a slightly lower temperature of 33.5°C with 5% CO2. SV-HUC-1, UMUC3, T24, 5637, J82 cells were obtained from Shanghai Institute of Cell Science, Chinese Academy of Sciences.

Quantitative Real-Time PCR (qRT-PCR) Assay

We measured gene expression levels using quantitative real-time PCR (qRT-PCR), and extracted total RNA using the TRIzol protocol stipulated by Vazyme. The subsequent reverse transcription process was executed with unwavering fidelity to the guidelines provided in the PrimeScript™ RT Kit (Takara, Japan). The primer sequences are shown in Table 1.

siRNA Transfection

The cells were categorized into three distinct groups: the siNC group, the siAHCY-1 group, and the siAHCY-2 group. The experimental procedure was meticulously structured as follows: 5637 cells were seeded into a 12-well plate. Upon reaching approximately 50% confluence, the cells were subjected to transient transfection in accordance with the aforementioned grouping and the detailed protocol provided by the manufacturer. The cells were transfected using DMEM and Lipofectamine RNAiMAX (Invitrogen, Waltham, MA, USA).

Forty-eight hours post-transfection, the efficiency of this crucial process was subjected to a rigorous evaluation, a critical step in ensuring the validity of the subsequent results. The siRNA primers instrumental to this study, sourced from GenePharma. The sequences of the si-RNA was shown in Table 2.

Cell Viability Assay

Following the siRNA transfection, a period of intense monitoring commenced, with cells being meticulously observed at predefined intervals of 24, 48, 72, and 96 hours, thereby facilitating a comprehensive temporal analysis of cellular

Table 1 Sequences of the PCR Primers

Gene	Primer
AHCY	Forward: 5′-ATCCTTGGCCGGCACTTTGAG-3′
	Reverse: 5′-TCCACCTGCGGCTTGATGTTC-3′
GAPDH	Forward: 5′-GGAGCGAGATCCCTCCAAAAT-3′
	Reverse: 5′-GGCTGTTGTCATACTTCTCATGG-3′
ZC3H13	Forward: 5′-TCTGATAGCACATCCCGAAGA-3′
	Reverse; 5′-CAGCCAGTTACGGCACTGT-3′
IGF2BP2	Forward: 5′- GTTCCCGCATCATCACTCTTAT-3′
	Reverse: 5′-GAATCTCGCCAGCTGTTTGA-3′
IGF2BP3	Forward: 5′-TCGTGACCAGACACCTGATGAG-3′
	Reverse: 5′-GGTGCTGCTTTACCTGAGTCAG-3′
ALKBH5	Forward: 5′-CCAGCTATGCTTCAGATCGCCT-3′
	Reverse: 5′-GGTTCTCTTCCTTGTCCATCTCC-3′

https://doi.org/10.2147/CMAR.S491044

Table 2 Sequences of the siRNA

Gene	Primer
siAHCY-1	Sense:5′-AUGCCAUUGUGUGUAACAUUGTT-3′
	Antisense:5′-CAAUGUUACACACAAUGGCAUTT-3′
siAHCY-2	Sense:5′-GAGCUAAUGGCACCAACUUUGTT-3′
	Sense:5′-CAAAGUUGGUGCCAUUAGCUCTT-3′

response. Experimental groups, meticulously categorized based on these time points, underwent cell viability assessments utilizing the CCK8 kit.

Cell Migration

Post-grouping, as meticulously detailed previously, cells were carefully seeded into 6-well plates, transfected over a period of 48 hours, and subsequently cultured until reaching a confluence of 70%-80%. A precise scratch, executed with the tip of a 200 μL pipette, was introduced in the central area of each well's cell monolayer. Immediate microscopic observations, crucial for establishing baseline cellular morphology, were followed by a second round of observations after 24 hours, allowing for a thorough assessment of cell migration.

Transwell and Colony Formation Assay

Prior to its introduction into the specifically designated chamber of a 24-well plate, the matrix gel underwent a fastidious dilution process with a pre-chilled, serum-free medium, maintaining a precise ratio of 15:1. This chamber was subsequently subjected to a controlled incubation period of 2 hours at a thermostatically regulated temperature of 37°C. Following this initial incubation phase, 500 μL of serum was meticulously introduced into the culture medium residing within the chamber. Cellular components, having undergone resuspension in a serum-free medium, were then seeded at a carefully calculated density of 1×10^5 cells per well, in chambers either containing the matrix gel, specifically designated for the invasion assay, or devoid of the matrix gel. These setups were then subjected to a more extended incubation period of 24 hours at a consistent temperature of 37°C. Post-incubation, the cellular matter was fixed utilizing formaldehyde, effectively halting further biological activity and preserving the cellular morphology. This was followed by staining with a crystal violet solution, which served to enhance the visualization of the cellular structures and facilitate the identification of specific cellular components. A subsequent washing with PBS served to remove any unbound dye, ensuring clarity in the ensuing microscopic examination. Five distinct fields of view were randomly selected under the discerning lens of a high-power microscope, facilitating detailed observation and accurate enumeration of the cellular components. This entire experimental procedure was meticulously repeated three times to ensure reliability and reproducibility. For colony formation, cells were digested, transfected with Si-AHCY, and collected in a centrifuge tube, with each well in a 6-well plate receiving 500 cells. Each experimental group consisted of three replicate wells. The culture medium was refreshed every 48 hours, and after 14 days of culture, the cells were fixed and stained.

Statistical Analysis

The statistical analyses were conducted using R 3.6.3. The correlation matrix consisted of Spearman correlation coefficients. The Wilcoxon test was employed to compare the two groups. The K-M curve and Log rank test were employed to assess disparities in survival rates. A p-value less than 0.05 was deemed statistically significant. Data visualization was performed using GraphPad Prism 7 software (GraphPad Software, Inc., San Diego, CA, USA).

Results

AHCY Expression in BLCA

An analysis was conducted on the expression levels of AHCY across various pancarcinoma types through TCGA and GTEx databases. The findings revealed a substantial heterogeneity in AHCY expression among different tumor types (Figure 1A). Building upon the established significance of AHCY in malignancies, such as colorectal cancer, prostate

cancer, and glioblastoma, we aim to explore its potential role in BLCA. Figure 1B distinctly illustrates a marked upregulation of AHCY expression in BLCA tumor tissues. Notably, the mRNA expression of AHCY manifested a pronounced and consistent regulation across the preponderance of tumor tissues (Figure 1C). ROC curve analysis was used to determine the threshold of the number of positive tests for AHCY expression in tumor patients versus non-tumor patients (AUC=0.882, CI=0.840–0.924) (Figure 1D). Moreover, the expression levels of AHCY mRNA were quantified in both normal cell lines and BLCA cell lines. The expression level in 5637 cells exhibited a statistically significant elevation, diverging conspicuously from other BLCA cell lines as well as the normal bladder epithelial cell line SV-HUC-1 (Figure 1E). Furthermore, the cBioPortal map in the TCGA dataset was used to investigate the oncoprint localization of the AHCY gene in BLCA patients (Figure 1F).

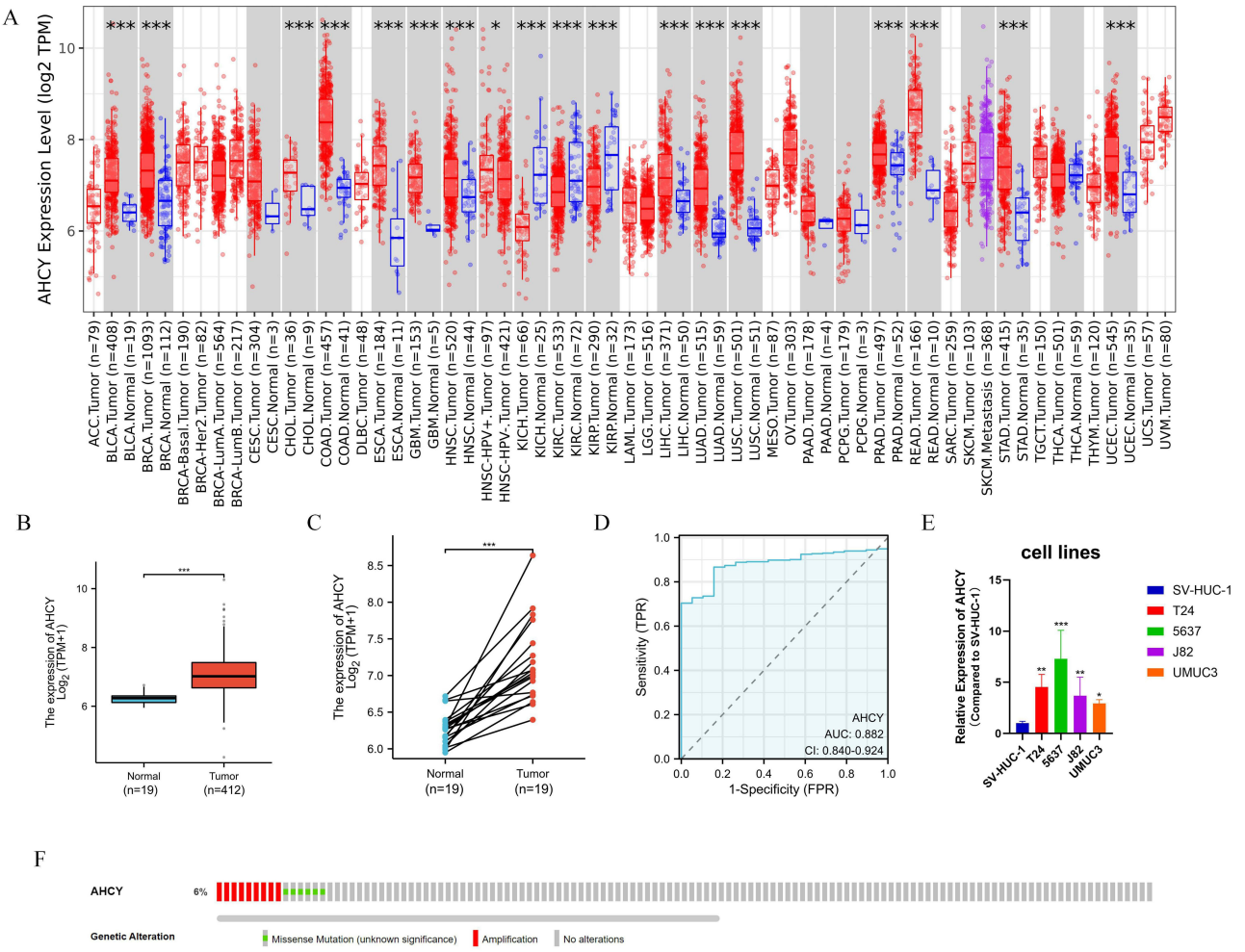

Figure 1 A comprehensive overview of the expression levels of AHCY across a wide spectrum of malignancies. (**A**) Elucidates the differential expression patterns of AHCY between normal and tumor samples in a diverse array of carcinoma subtypes, including ACC (adenoid cystic carcinoma), BLCA (bladder urothelial carcinoma), BRCA (breast invasive carcinoma), CESC (encompassing both cervical squamous cell carcinoma and endocervical adenocarcinoma), CHOL (cholangiocarcinoma), COAD (colon adenocarcinoma), DLBC (diffuse large B-cell lymphoma), ESCA (esophageal carcinoma), GBM (glioblastoma multiforme), HNSC (head and neck squamous cell carcinoma), KICH (kidney chromophobe), KIRC (kidney renal clear cell carcinoma), KIRP (kidney renal papillary cell carcinoma), LAML (acute myeloid leukemia), LGG (brain lower grade glioma), LIHC (liver hepatocellular carcinoma), LUAD (lung adenocarcinoma), LUSC (lung squamous cell carcinoma), MESO (mesothelioma), OV (ovarian serous cystadenocarcinoma), PAAD (pancreatic adenocarcinoma), PCPG (pheochromocytoma and paraganglioma), PRAD (prostate adenocarcinoma), READ (rectum adenocarcinoma), SARC (sarcoma), SKCM (skin cutaneous melanoma), STAD (stomach adenocarcinoma), TGCT (testicular germ cell tumors), THCA (thyroid carcinoma), THYM (thymoma), UCEC (uterine corpus endometrial carcinoma), UCS (uterine carcinosarcoma), and UVM (uveal melanoma). (**B**) A examination of AHCY expression levels in BLCA and adjacent normal tissues. (**C**) The quantification of AHCY mRNA expression levels was performed via qRT-PCR in SV-HUC-1 and a diverse array of BLCA cell lines. (**D**) The expression patterns of AHCY in BLCA and corresponding normal tissues were examined. (**E**) The cBioPortal OncoPrint map provides a comprehensive illustration of the distribution of AHCY genomic alterations among BLCA patients. (**F**) The cBioPortal OncoPrint map provides a comprehensive illustration of the distribution of AHCY genomic alterations among BLCA patients. *, ** and *** indicate p<0.05, p<0.01 and p < 0.001.

https://doi.org/10.2147/CMAR.S491044

The Correlation Between the Expression Level of AHCY and Clinicopathological Characteristics in Patients with BLCA

The relationship between clinical parameters and AHCY expression levels in BLCA patients was examined using the TCGA database. These clinical parameters encompassed gender, age, pathologic T stage, pathologic N stage, pathologic M stage, pathologic stage, weight, subtype, histologic grade, OS event, DSS event and PFI event (Figure 2A–G). Our study found that the expression of AHCY was highly relevant to subtype (Figure 2H), histologic grade (Figure 2I), OS event (Figure 2J), DSS event (Figure 2K), and PFI event (Figure 2L). These results emphasize the correlation between AHCY expression and numerous clinical features of BLCA.

AHCY Affects the Prognosis of BLCA Patients

To elucidate the ramifications of AHCY expression on patient survival, BLCA patients was stratified into two distinct groups predicated on their respective levels of AHCY expression. The initial group encompassed the top 50% of the samples that manifested the high levels of AHCY expression, whereas the latter group included the inferior 50%, showcasing low expression levels. Subsequently, an survival analysis was undertaken, employing the mean expression value of AHCY as a pivotal reference point. Utilizing the Kaplan-Meier survival analysis technique, we found that elevated AHCY expression was linked with deleterious outcomes in BLCA patients.

This phenomenon was especially conspicuous with regard to overall survival and progression-free survival (Figure 3A and B). In the next analysis, subgroup evaluations were conducted on BLCA patients across various clinicopathological states. It was ascertained that elevated AHCY expression exhibited a substantial correlation with

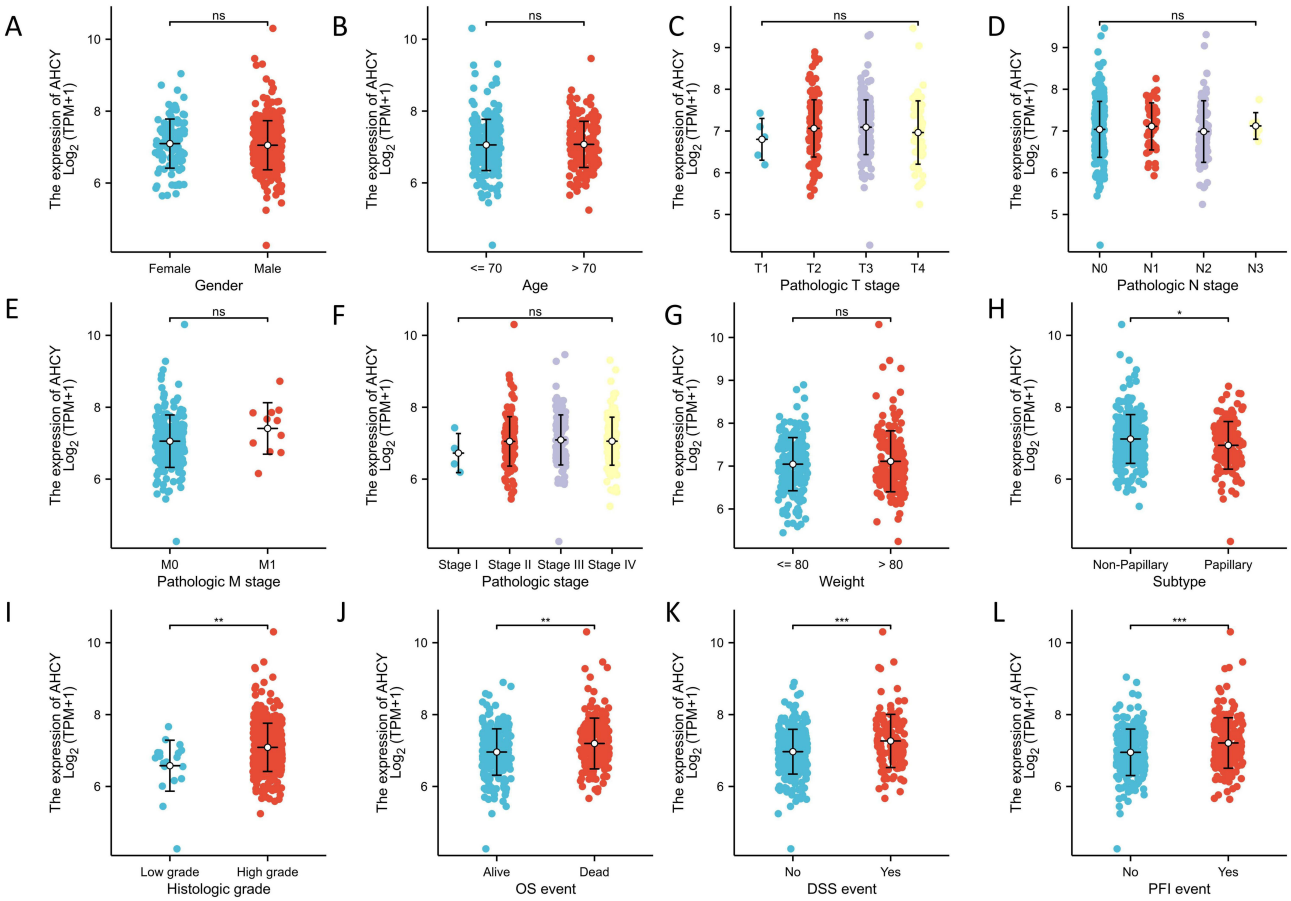

Figure 2 Expression level of AHCY in tumor tissues of patients with different clinical characteristics. The relationship between Gender (**A**), Age (**B**), Pathologic T stage (**C**), Pathologic N stage (**D**), Pathologic M stage (**E**), Pathologic stage (**F**), Weight (**G**), Subtype (**H**), Histologic grade (**I**), OS event (**J**), DSS event (**K**), PFI event (**L**) and AHCY. *, ** and *** indicate $p<0.05$, $p<0.01$ and $p < 0.001$.

https://doi.org/10.2147/CMAR.S491044

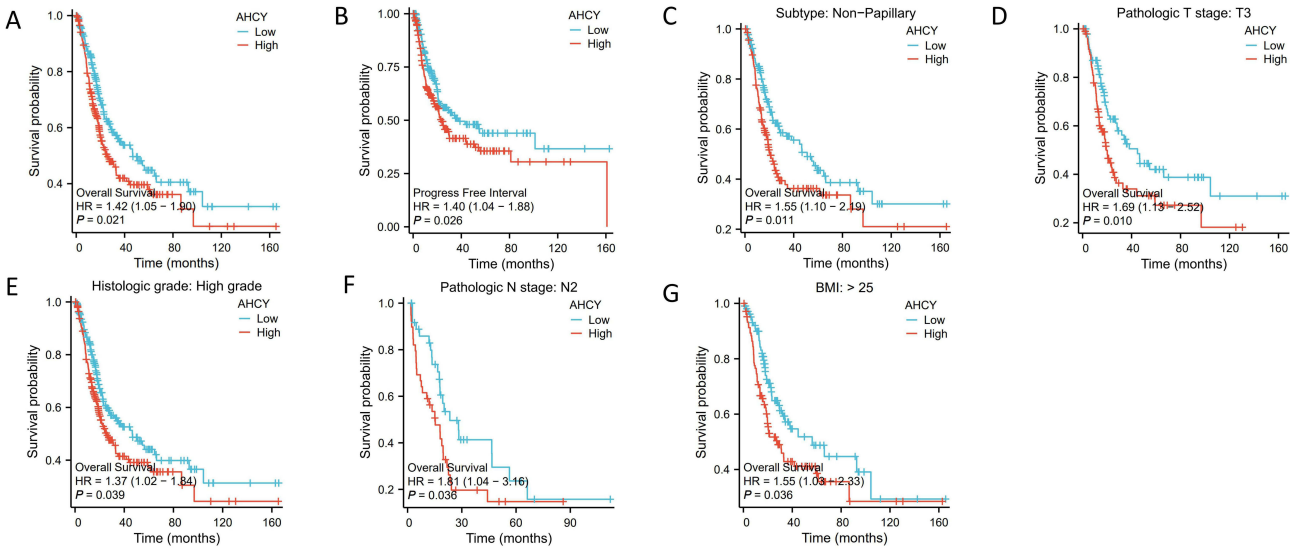

Figure 3 The Correlation Between AHCY Expression and Bladder Cancer Prognosis. (**A** and **B**) The relationship between AHCY expression levels and overall survival (OS) and progression free survival (PFS) in BLCA patients. (**C-G**) The impact of AHCY expression on prognosis in different patient subgroups including pathologic T stage, histologic grade, pathologic N stage, BMI and subtype.

an unfavorable prognosis in BLCA, permeating various demographic and clinical subgroups. This included those with stage T3 tumors, high-grade neoplasms, node-positive status N2, individuals presenting with a BMI surpassing 25, as well as non-papillary tumor morphology (Figure 3C–G).

An Elevated Expression of AHCY Was a Distinct Risk Factor for Overall Survival of BLCA

The prognosis of BLCA was evaluated through both univariate and multivariate Cox proportional hazards regression analyses. The independent variables scrutinized encompassed gender, pathological N stage, subtype, age, pathological T stage, pathological M stage, and AHCY expression. Notably, the analysis indicated that an high expression of AHCY emerged as a significant predictor of overall survival in BLCA patients. Furthermore, both univariate and multivariate analyses convergently underscored the pathological N stage as a potent prognostic factor for overall survival in patients with BLCA. Additionally, the univariate analysis identified subtype, age, pathological T stage, and pathological M stage as pivotal prognostic factors (Table 3).

Construction of Prognostic Line Graph Based on Independent Prognostic Factors

Subsequently, a nomogram is constructed by incorporating independent prognostic markers, including pathologic N stage, pathologic T stage, pathologic M stage, subtype, age, and AHCY. The association between six clinicopathological characteristics (pathologic N stage, pathologic T stage, pathologic M stage, subtype, age, and AHCY) and the survival rates of OS at 1-year, 3-year, and 5-year intervals (Figure 4A). The calibration curves at 1-year, 3-year, and 5-year intervals demonstrate concordance between our findings and the projected values, hence suggesting a reasonable level of performance for the nomogram based on AHCY (Figure 4B). The c index value of 0.651 suggests a moderate level of accuracy in the predictions.

Functional Enrichment of AHCY-Related Genes

The Limma software tool was employed to execute a differential expression analysis contrasting conditions of low and high AHCY. A curated cohort of 714 differential genes was selected, adhering to the stringent criteria of |logFC| >1 and a statistically significant adjusted p-value (Figure 5A). This cohort was composed of 402 genes identified as up-regulated and 312 as down-regulated. Subsequently, we exam the genes coexpressed in correlation with AHCY expression within

https://doi.org/10.2147/CMAR.S491044

Table 3 Univariate and Multivariate Cox Regression Analysis of BLCA OS-Related Clinical Features in TCGA Patients

Characteristics	Total (N)	Univariate Analysis		Multivariate Analysis	
		HR (95% CI)	p value	HR (95% CI)	p value
Gender	411				
Female	108	Reference			
Male	303	0.868 (0.629–1.198)	0.39		
Pathologic N stage	367				
N0	238	Reference		Reference	
N1&N2&N3	129	2.250 (1.649–3.072)	< 0.001	1.955 (1.165–3.280)	0.011
Subtype	406				
Non-Papillary	273	Reference		Reference	
Papillary	133	0.690 (0.487–0.976)	0.036	0.845 (0.477–1.495)	0.562
Age	411				
<= 70	231	Reference		Reference	
> 70	180	1.424 (1.064–1.906)	0.018	1.207 (0.745–1.955)	0.445
Pathologic T stage	377				
T1&T2	123	Reference		Reference	
T3&T4	254	2.157 (1.485–3.132)	< 0.001	1.949 (0.997–3.807)	0.051
Pathologic M stage	212				
M0	201	Reference		Reference	
M1	11	3.112 (1.491–6.493)	0.002	1.544 (0.578–4.126)	0.387
AHCY	411				
Low	205	Reference		Reference	
High	206	1.416 (1.054–1.903)	0.021	1.559 (0.955–2.544)	0.076

the TCGA BLCA dataset. We selected 2236 genes with a Spearman correlation coefficient exceeding 0.3 and a p-value below 0.05. Figure 5B delineates the 35 genes exhibiting the most pronounced positive correlations. The analysis revealed the intricate involvement of genes co-expressed with AHCY in a vast and diverse array of 817 biological processes, 238 cellular components, 184 molecular functions, and 43 KEGG pathways. The GO term indicates that these genes are implicated in a wide spectrum of biological processes. Furthermore, these genes contribute to mitochondrial inner membrane functionality, single-stranded DNA binding, and ribonucleoprotein complex binding (Figure 5C–E).

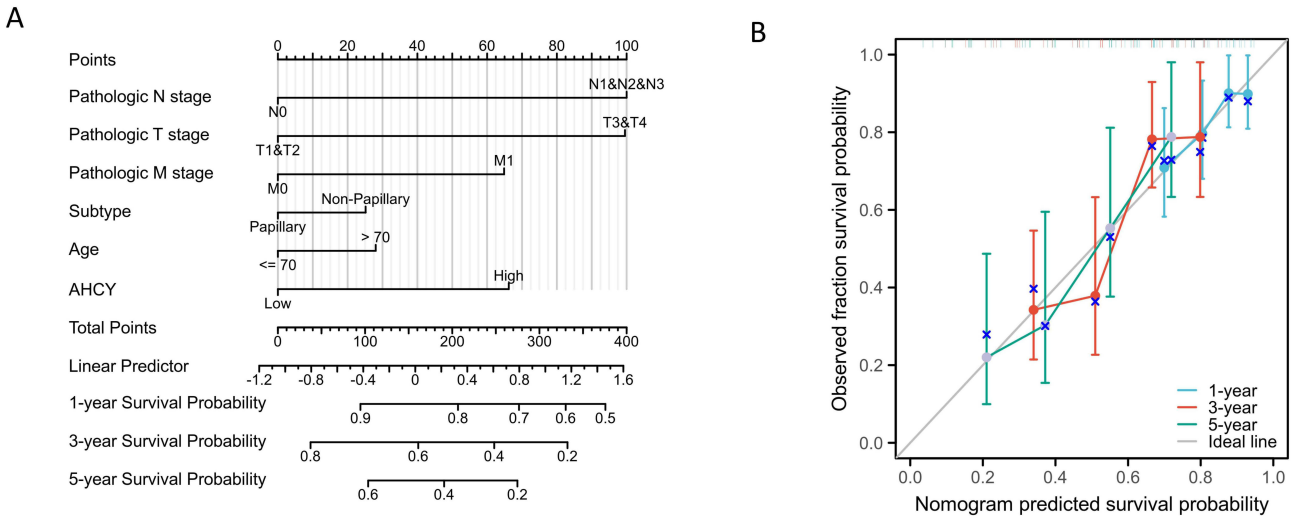

Figure 4 Construction of prediction line chart. (**A**) Nomograms to predict OS 1, 3, and 5 years. (**B**) 1-year, 3-year and 5-year correction curves.

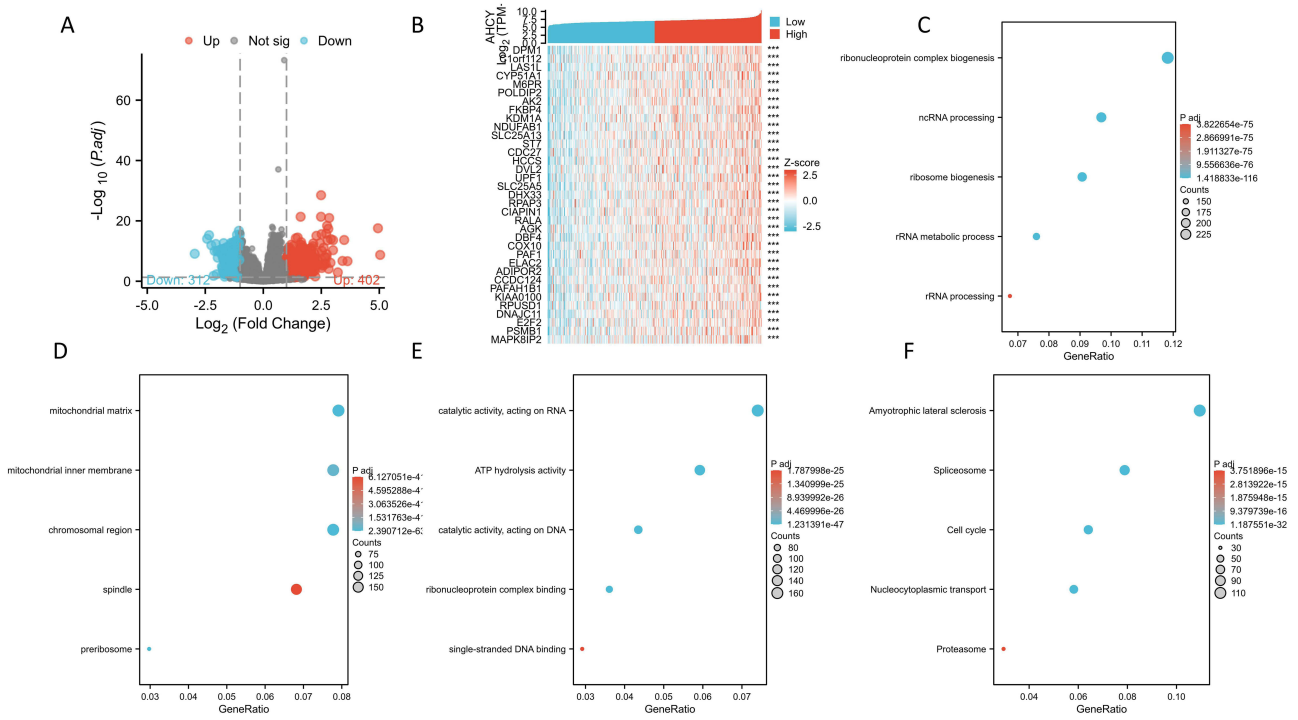

Figure 5 Functional Clustering and Interaction Network Analysis of AHCY-Related Genes. (**A**) Volcanic plot illustrating differentially expressed genes. (**B**)The heatmap delineates the top 35 genes in BLCA that exhibit a positive correlation with AHCY. (**C**) Biological Process (BP) enrichment analysis of genes coexpressed with AHCY. (**D**) Cellular Component (CC) enrichment analysis of genes coexpressed with AHCY. (**E**) Molecular Function (MF) enrichment analysis of genes coexpressed with AHCY. (**F**) Enrichment analysis of AHCY co-expressed genes within the KEGG pathways. *** indicates $p < 0.001$.

These genes were implicated in critical pathways such as amyotrophic lateral sclerosis, the spliceosome, cell cycle regulation, nucleocytoplasmic transport, and the proteasome (Figure 5F). The comprehensive GO terminology and KEGG pathway data pertinent to the AHCY co-expression enrichment study are concisely summarized in Supplementary materials.

Relationship Between AHCY Expression Level and m6A Modification in BLCA

The primary focus of functional enrichment of genes associated with AHCY pertains to biological activities, including rRNA processing, ncRNA processing, and ribosome biogenesis. M6A RNA methylation is crucial for RNA synthesis. Consequently, we hypothesized that the degree of AHCY expression could be associated with the alteration of m6A. Subsequently, a examination was undertaken to elucidate the correlation between the expression levels of AHCY in BLCA and 20 genes implicated in m6A modifications. The expression of AHCY is positively correlated with important genes in the m6A modification pathway, including YTHDF1, YTHDF2, YTHDF3, YTHDC1, YTHDC2, WTAP, RBM15, RBM15B, HNRNPC, METTL14, METTL3, IGF2BP2, RBMX, HNRNPA2B1, VIRMA, FTO, and ALKBH5 (Figure 6A and B). The analysis indicate the expression of the AHCY is significantly correlated with lots of genes, including YTHDF1, YTHDF3, RBM15, HNRNPC, RBMX, HNRNPA2B1, VIRMA, and ALKBH5. We found that high expression of genes ZC3H13, IGF2BP2, IGF2BP3, and ALKBH5 in BLCA can lead to poor prognosis (Figure 6C).

Correlation Between AHCY Expression and Immune Characteristics

Utilizing TCGA database, our study unveiled a positive association between the expression of AHCY in BLCA patients and the presence of Th2 cells and Tgd cells. Conversely, a negative correlation between the expression of AHCY and pDC, Mast cells, iDC, and DC (Figure 7A). Further investigations, our found a positive correlation between AHCY expression and the infiltration of Th2 cells, as vividly illustrated in Figure 7B, as well as with Tgd cells, as depicted in Figure 7C. Notably, there are differences in the infiltration levels of Th2 cells and Tgd cells between patients with high

https://doi.org/10.2147/CMAR.S491044

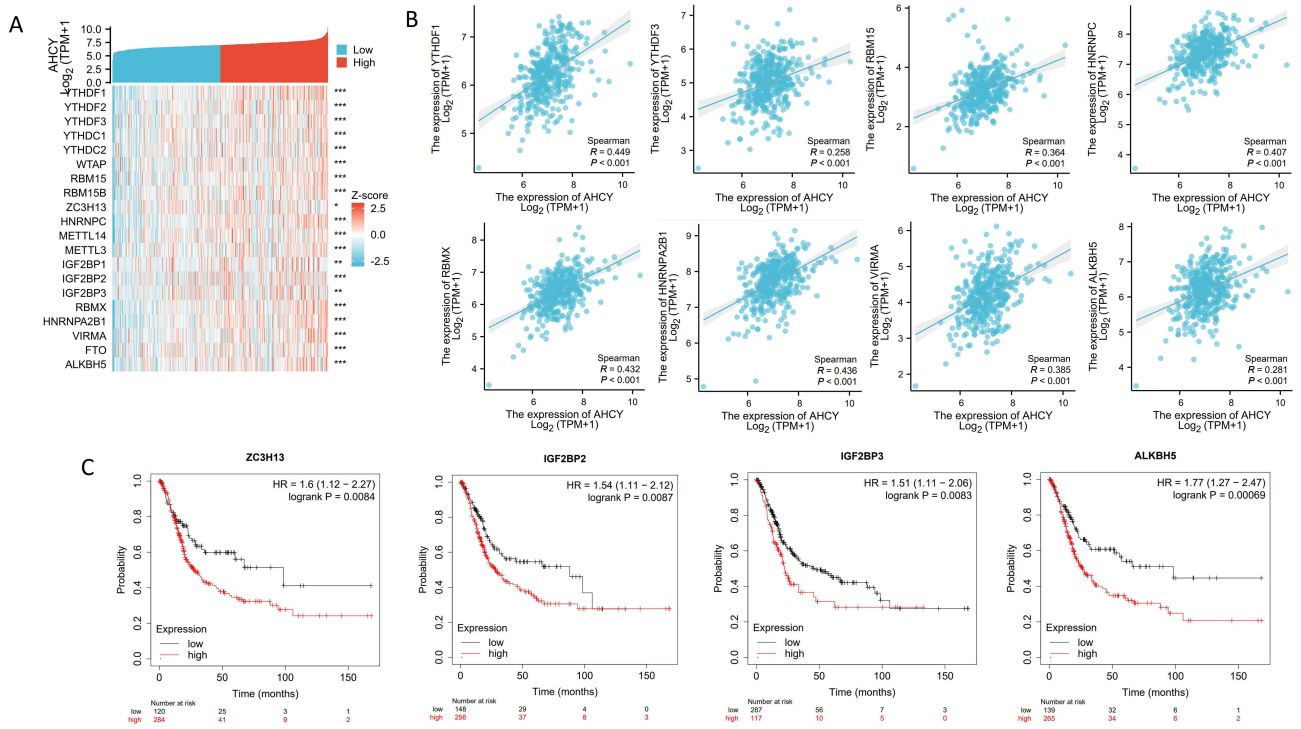

Figure 6 Interplay between AHCY Expression and m6A-Associated Genes in BLCA. (**A**) An analysis was conducted to elucidate the correlation between AHCY and a suite of 20 m6A-related genes within the TCGA BLCA cohort. (**B**) A scatterplot illustrates the intricate dynamics between AHCY expression and the levels of m6A-associated genes. (**C**) The prognostic significance of ZC3H13, IGF2BP2, IGF2BP3, and ALKBH5 in the context of BLCA was evaluated. *, ** and *** indicate p<0.05, p<0.01 and p < 0.001.

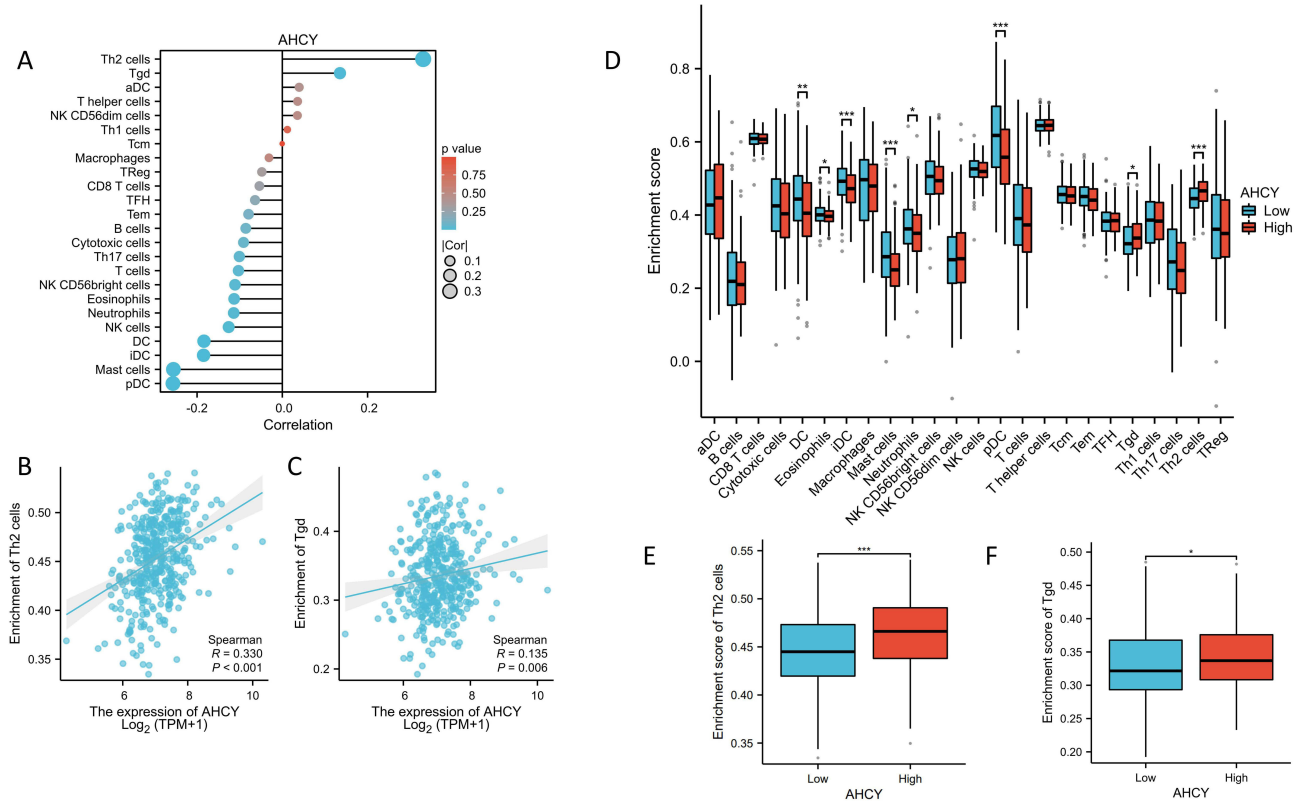

Figure 7 Correlation Analysis of AHCY Expression and Immunoinfiltration in BLCA. (**A**) The relationship between AHCY and immunoinfiltrating cells in BLCA patients. (**B**) The correlation between AHCY expression and Th2 cell infiltration levels via a scatter plot. (**C**) The correlation between AHCY expression and Tgd cell infiltration levels via a scatter plot. (**D**) The differences in immune cell distribution between patients with high and low AHCY expression. (**E** and **F**) Differences in levels of Th2 cell and Tgd cell infiltration between high and low AHCY expression cohorts. *, ** and *** indicate p<0.05, p<0.01 and p < 0.001.

https://doi.org/10.2147/CMAR.S491044

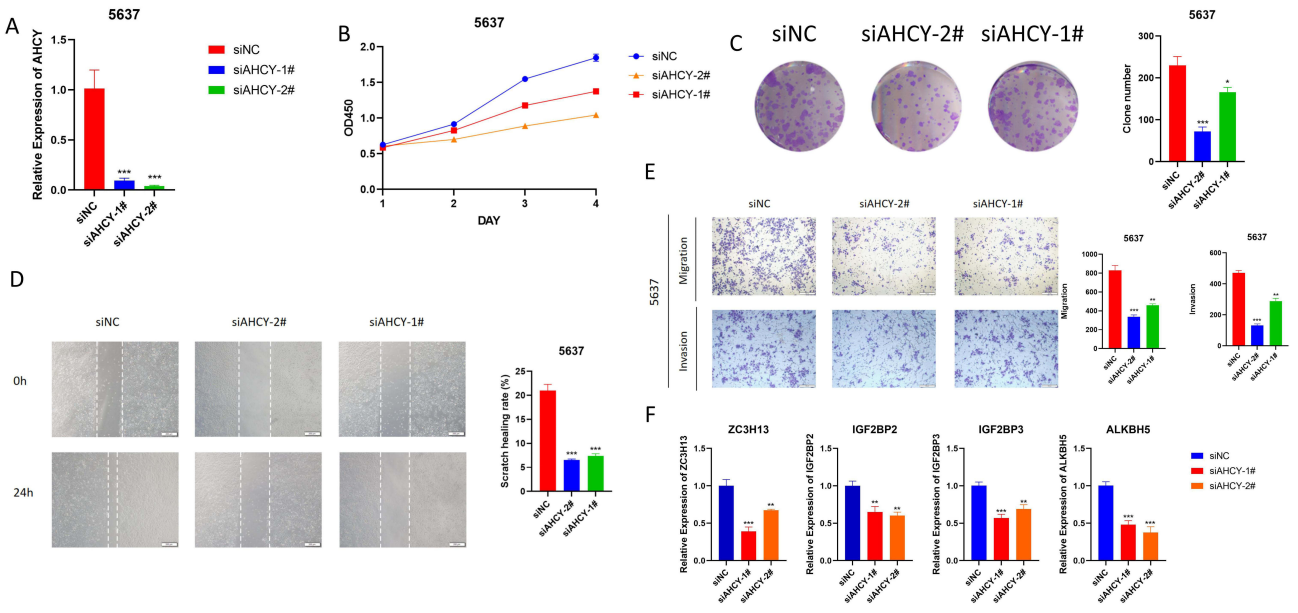

Figure 8 The effects of AHCY on the proliferation, migration, invasion and anti-apoptosis of bladder cancer were verified in vitro. (**A**) qPCR compare AHCY mRNA content between the knockdown group and the control group. (**B**)The proliferation ability of 5637 cells with si-AHCY and of si-NC. (**C**) Compared the colony formation of 5637 cells with si-AHCY or si-NC. (**D**) Compared the migration efficiency of 5637 cells in 0 and 24 hours between the si-NC and the si-AHCY group (scale of 200um). (**E**) The invasive ability of 5637 cells was examined by Transwell assay (scale of 100um). (**F**) Relative mRNA expression of ZC3H13, IGF2BP2, IGF2BP3, and ALKBH5 in BLCA after knocking down AHCY. *, ** and *** indicate $p<0.05$, $p<0.01$ and $p < 0.001$.

and low AHCY expression (Figure 7D–F). Significantly, this data reveal that AHCY maintains a profound correlation with Th2 cells and Tgd cells, underscoring its potential role in modulating immune dynamics within BLCA.

Knockdown of AHCY Inhibited the Proliferation, Migration, Invasion of BLCA Cells

The strong expression of AHCY in BLCA cells (5637 cells) was confirmed in previous q-PCR investigations, therefore leading us to select 5637 cells for verification purposes (Figure 1D). The qPCR results indicated that si-AHCY-2# exhibited a greater knockdown efficiency (Figure 8A). Subsequent cell research utilized this si-RNA. The results elucidated that the targeted suppression of AHCY precipitated a diminution in the proliferative capabilities of 5637 cells (Figure 8B). Furthermore, the inhibition of AHCY engendered a decrement in the clonogenic potential of these cells (Figure 8C). Concomitantly, the scratch healing rate of 5637 cells was observed to undergo a attenuation subsequent to the AHCY knockout (Figure 8D). Additionally, the silencing of AHCY was associated with a pronounced reduction in the migratory and invasive capacities of 5637 cells (Figure 8E). Moreover, we found the mRNA levels of ZC3H13, IGF2BP2, IGF2BP3 and ALKBH5 were all reduced to varying degrees after AHCY knockdown (Figure 8F).

Discussion

By using the TCGA database, our study found positive correlation between the expression levels of AHCY and both the specific subtype and histologic grade of the BLCA This observation intimates that AHCY may indeed assume a critical role in the aggressive proliferation and invasive behavior of BLCA, warranting further investigation into its potential as a therapeutic target. Further scrutinizing our analysis of OS, progression-free survival and survival rates across diverse subgroups has yielded evidence: patients exhibiting augmented expression of AHCY, has been identified as diminished survival rates. These findings reported the importance of AHCY in predicting disease outcomes. Taken together, the findings of our investigation consistently substantiate the proposition that AHCY holds promise as a reliable prognostic biomarker for BLCA diagnosis.

In an effort to provide a more comprehensive investigation into the multifaceted biological role of AHCY in BLCA, we conducted a meticulous functional enrichment analysis on genes that are associated with AHCY expression. It is reported that the m6A alterations are widely prevalent and often occurring RNA changes that have the potential to impact

the advancement of tumors and the spread of cancer by modulating the expression of many genes associated with cancer.[14] Consequently, we postulate that the expression levels of AHCY might be linked with modifications in m6A dynamics. Through our research, a significant correlation between the expression of AHCY and twenty genes associated with m6A was discerned within the context of BLCA. The overexpression of IGF2BP3 in individuals diagnosed with BLCA was associated with an adverse prognosis.[15] Furthermore, the genes PGM1 and ENO1 manifest a robust positive correlation with the malignant progression of BLCA.[16] Consequently, we postulate that AHCY may undergo significant modulation by aberrant m6A expression, thus influencing the trajectory of BLCA.

Due to the significant impact of TME on cancer progression, we designed a study to explain the relationship between AHCY expression and BLCA immune infiltration. The results indicate that a positive correlation between the expression of AHCY and the expression of Th2 cells and Tgd. Research has indicated that Th2 cells possess the ability to impede the proliferation of colon and pancreatic cancer through the facilitation of the anti-tumor reaction of macrophages and eosinophils.[17] TME exhibits a unique metabolic interdependence with Th2 cells in cancer treatment. These findings indicate that AHCY may exert an influence on the metabolic alterations inside the TME via Th2 cells and Tgd, hence impacting the incidence and progression of BLCA.

Through in vitro tests, we observed that the suppression of AHCY had a substantial inhibitory effect on the growth, movement, and infiltration in 5637 cells. These results are consistent with our previous research.

Nevertheless, the study is not without its limitations. Our data is sourced from public databases and there may be deviations. Furthermore, it is necessary to further validate my data through in vivo and in vitro experiments.

Conclusions

This investigation represents the inaugural inquiry into the prognostic significance of AHCY in BLCA. Our findings suggest that AHCY is a potential biomarker for forecasting treatment outcomes and prognoses in BLCA patients.

Data Sharing Statement

The study encapsulates original findings, accessible within the body of the article or the Supplementary Material. Additional inquiries regarding the data should be directed towards the respective authors.

Acknowledgment

We acknowledge TCGA, GTEx, TIMER database, GEPIA database, CIBERSORT algorithm, ESTIMATE algorithm for providing their platforms and contributors for uploading their meaningful datasets, and all the patients who gave consent to disclose their medical records.

Author Contributions

All authors made a significant contribution to the work reported, whether that is in the conception, study design, execution, acquisition of data, analysis and interpretation, or in all these areas; took part in drafting, revising or critically reviewing the article; gave final approval of the version to be published; have agreed on the journal to which the article has been submitted; and agree to be accountable for all aspects of the work.

Disclosure

Dr Jiaxue Yang reports grants from The Third Affiliated Hospital of Nanchang University, during the conduct of the study. The authors report no other conflicts of interest in this work.

References

1. Kusakabe Y, Ishihara M, Umeda T, et al. Structural insights into the reaction mechanism of S-adenosyl-L-homocysteine hydrolase. *Sci Rep*. 2015;5 (16641). doi:10.1038/srep16641.
2. Santiago L, Daniels G, Wang D, Deng FM, Lee P. Wnt signaling pathway protein LEF1 in cancer, as a biomarker for prognosis and a target for treatment. *Am J Cancer Res*. 2017;7(6):1389–1406.
3. Ducker GS, Rabinowitz JD. One-carbon metabolism in health and disease. *Cell Metab*. 2017;25(1):27–42. doi:10.1016/j.cmet.2016.08.009

4. Uchiyama N, Tanaka Y, Kawamoto T. Aristeromycin and DZNeP cause growth inhibition of prostate cancer via induction of mir-26a. *Eur J Pharmacol*. 2017;812:138–146.
5. Li Y, Zheng X, Wang J, et al. Exosomal circ-AHCY promotes glioblastoma cell growth via Wnt/β-catenin signaling pathway. *Ann Clin Transl Neurol*. 2023;10(6):865–878. doi:10.1002/acn3.51743
6. Sung H, Ferlay J, Siegel RL, et al. Global cancer statistics 2020: GLOBOCAN estimates of incidence and mortality worldwide for 36 cancers in 185 countries. *CA Cancer J Clin*. 2021;71(3):209–249. doi:10.3322/caac.21660
7. Abudurexiti M, Ma J, Li Y, et al. Clinical outcomes and prognosis analysis of younger bladder cancer patients. *Curr Oncol*. 2022;29(2):578–588. doi:10.3390/curroncol29020052
8. Mao X, Xu J, Wang W, et al. Crosstalk between cancer-associated fibroblasts and immune cells in the tumor microenvironment: new findings and future perspectives. *mol Cancer*. 2021;20(1):131. doi:10.1186/s12943-021-01428-1
9. Wang Y, Huang T, Gu J, Lu L. Targeting the metabolism of tumor-infiltrating regulatory T cells. *Trends Immunol*. 2023;44(8):598–612. doi:10.1016/j.it.2023.06.001
10. Barkley D, Moncada R, Pour M, et al. Cancer cell states recur across tumor types and form specific interactions with the tumor microenvironment. *Nat Genet*. 2022;54(8):1192–1201. doi:10.1038/s41588-022-01141-9
11. Sun T, Wu R, Ming L. The role of m6A RNA methylation in cancer. *Biomed Pharmacother*. 2019;112(108613):108613. doi:10.1016/j.biopha.2019.108613
12. An Y, Duan H. The role of m6A RNA methylation in cancer metabolism. *mol Cancer*. 2022;21(1):14. doi:10.1186/s12943-022-01500-4
13. Ni Z, Sun P, Zheng J, et al. JNK signaling promotes bladder cancer immune escape by regulating METTL3-mediated m6A modification of PD-L1 mRNA. *Cancer Res*. 2022;82(9):1789–1802. doi:10.1158/0008-5472.CAN-21-1323
14. Zhuang H, Yu B, Tao D, et al. The role of m6A methylation in therapy resistance in cancer. *mol Cancer*. 2023;22(1):91. doi:10.1186/s12943-023-01782-2
15. Huang W, Zhu L, Huang H, Li Y, Wang G, Zhang C. IGF2BP3 overexpression predicts poor prognosis and correlates with immune infiltration in bladder cancer. *BMC Cancer*. 2023;23(1):116. doi:10.1186/s12885-022-10353-5
16. Zhao J, Huang S, Tan D, et al. PGM1 and ENO1 promote the malignant progression of bladder cancer via comprehensive analysis of the m6A signature and tumor immune infiltration. *J Oncol*. 2022;2022:8581805.
17. Jacenik D, Karagiannidis I, Beswick EJ. Th2 cells inhibit growth of colon and pancreas cancers by promoting anti-tumorigenic responses from macrophages and eosinophils. *Br J Cancer*. 2023;128(2):387–397. doi:10.1038/s41416-022-02056-2